Sensors & Actuators: A. Physical 392 (2025) 116711

Contents lists available at ScienceDirect

Sensors and Actuators: A. Physical

journal homepage: www.journals.elsevier.com/sensors-and-actuators-a-physical

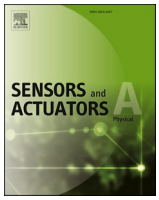

Modeling and modification of fin-ray effect grippers to improve their load capacity and grasp stability

Mohammad Sheikh Sofla [a,*], Hanita Golshanian [a], Elizabeth I. Sklar [a], Marcello Calisti [a,b]

[a] School of Agri-food Technology and Manufacturing, University of Lincoln, Lincoln, UK
[b] The BioRobotics Institute, Scuola Superiore Sant'Anna, Pisa, Italy

ARTICLE INFO

Keywords:
Fin-ray effect gripper
Cosserat rod theory
Grasp stability
Load capacity

ABSTRACT

Fin-ray effect (FRE) grippers are very popular because they can passively adapt to different shapes and therefore grasp a variety of objects. To optimize them for different purposes, in-depth analysis of their deformations and internal forces is required, which necessitates accurate mathematical models. This paper presents a modeling framework that improves upon existing approaches by representing all structural components of the FRE finger as Cosserat rods, capturing their continuum behavior. The static forward kinematics problem for these fingers is formulated as the solution to multiple Cosserat rod models with coupled boundary conditions, and the experimental investigations verified the accuracy of the proposed modeling method. Then, simulations were performed to investigate the effects of different design parameters on the grasp forces and conforming to the shape of objects. By defining new boundary conditions, the FRE fingers in simulation could apply more grasp forces and better envelop the objects. Thus, a new mounting adaptor was designed based on the proposed boundary conditions, and the experimental investigations revealed that the modified design could improve the load capacity by up to 150 % and provide more stable grasps for delicate objects in a wide range of shapes and sizes.

1. Introduction

Over the past decade, researchers have investigated the employment of soft and elastic materials to build robotic systems [1–4]. These robots often mimic the flexibility and adaptability of biological organisms, allowing them to interact with their environment in unique and versatile ways [5–7]. Fin ray effect (FRE) grippers are inspired by the natural movement of fish fins and can adapt to different object shapes and sizes [8,9]. Their soft and compliant structure allows them to conform to irregular or complex objects and enables them to handle delicate or fragile objects with care. This makes them well-suited for applications where gentle manipulation is required, such as handling biological specimens or delicate components [10]. Their compliant nature can reduce the risk of damage to objects or injury to humans in collaborative robotic applications. Moreover, the lightweight and compact nature of these grippers can reduce the overall weight of robotic systems and allow for easier integration into various platforms.

Due to these advantages, FRE grippers are increasingly gaining attention and finding applications in areas such as industrial automation [11–13], biomedical engineering [14], and human-robot interaction [15,16]. Their ability to combine adaptability with gentle and precise handling makes them a promising solution for various challenging tasks in robotics and automation [17,18].

However, FRE grippers, like most soft grippers, are better suited for handling lighter loads compared to traditional rigid grippers. The compliant and flexible nature of the fins, which allows them to deform around an object, limits the maximum load they can carry and decreases their grasp stability for fast robotic maneuvers. The load capacity of a FRE gripper depends on various factors including the design of the finger, the material properties, the mounting adaptor, and the utilized actuation mechanism. This research aims to analyze and optimize these grippers to provide more stable grasps and higher load-carrying capacities.

FRE fingers can be easily customized for different purposes by adjusting the shape, size, and arrangement of the fins [19–21], as well as the mounting adaptor design. This flexibility allows for modifying the gripper to specific tasks or object types. However, a proper accurate model is needed to analyze the shape and the internal forces when varying different design parameters. With a proper model, one can explore optimization techniques to enhance the gripper's performance

* Corresponding author at: School of Agri-food Technology and Manufacturing, University of Lincoln, Lincoln, UK
E-mail addresses: msofla@lincoln.ac.uk (M.S. Sofla), hgolshanian@lincoln.ac.uk (H. Golshanian), esklar@lincoln.ac.uk (E.I. Sklar), marcello.calisti@santannapisa.it (M. Calisti).

https://doi.org/10.1016/j.sna.2025.116711
Received 2 December 2024; Received in revised form 5 May 2025; Accepted 18 May 2025
Available online 21 May 2025

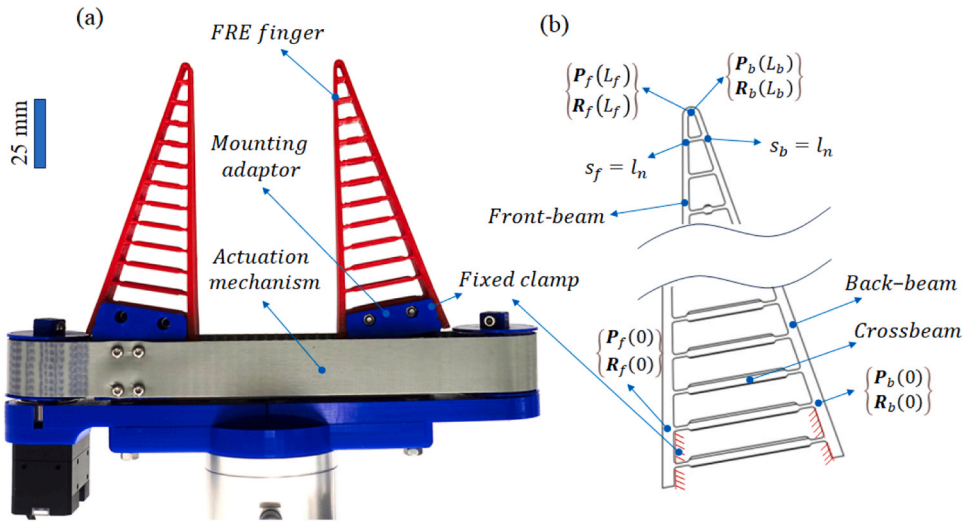

Fig. 1. (a) A prototype of the FRE gripper with the original mounting adaptor and (b) schematic of its boundary conditions.

for different applications. Some discretized models have been proposed for these fingers. In [22], a mathematical formulation based on the discrete Cosserat approach and assuming piecewise constant strains (PCS) is proposed for the analysis of closed-chain soft robots and is applied to the FRE structures. The crossbeams were designed as rigid links being connected with the front- and back-beams by revolute joints. Compared with the FRE fingers with rigid crossbeams, the benefits of integrated design with soft materials include having no sliding parts (and therefore no friction or stick-slip effects), no backlash, more compliant structure, and simplified fabrication process. In [23], to analyze the kineto-static behavior of the FRE fingers with integrated soft crossbeams, a Pseudo Rigid Body (PRB) model was introduced that considered the main beams as several phalanges connected by revolute joints to each other. The crossbeams are also considered as rigid links connected by revolute joints to the main beams. The continuum deformation of the beams was ignored in this study to simplify the modeling process that was the main source of error. This simplification also affects the analysis of various arrangements of the beams and their influence on grasping performance.

The present research aims to consider the continuum deformation of all beams in the soft FRE fingers. Cosserat rod theory, as a comprehensive and accurate modelling method for continuum beams, has been investigated in recent studies and found applications in various fields including biomechanics [24], robotics [25–27], textile engineering [28], and structural mechanics [29], where the accurate modeling of slender and flexible components is necessary. This modelling method considers extension, bending and twisting of the rods, and considers shear deformations that are crucial for modeling the behavior of slender structures. In this study, the beams of FRE fingers are independently described using the Cosserat rod theory, considering their coupled boundary conditions. The proposed model in this article facilitates the analysis of various shapes, sizes, and arrangements of the beams, as well as mounting adaptor designs, for the FRE fingers by flexible beams (integrated design with soft materials). We used the developed model to analyze and optimize this type of gripper.

Some researchers have focused on the improvement of the grasp performance of FRE fingers by structural optimization. In [18], a FRE finger composed of both rigid and flexible materials was fabricated, and finite element analysis showed that the new finger can undergo a 15 % greater deformation than conventional FRE fingers when exposed to an equivalent force. An increased number of crossbeams tilted towards the contact surface was explored in [20], revealing that a layer jamming effect could be induced as the FRE finger grasps an object. This jamming effect increased the stiffness of the finger. In [30], a spring is employed to apply a gripping force to objects, based on the Festo FRE structure [31]. The study explores the grasp force and the dynamic reaction force directed upward while grasping, considering various incline angles of the crossbeams. The effects of modifying the rib geometry on FRE finger performance are explored in [32]. Results from finite element simulations indicated that configuring FRE fingers with ribs featuring circular curved slopes improves the conformity performance.

However, among all these studies, few works have analyzed the load capacity of the fingers, and none of them investigated the effect of a different mounting adaptor design. The potential for improving the grasp force of FRE fingers with various beam arrangements is limited. Therefore, the effect of various mountings by analyzing different boundary conditions for the main beams was explored in this study. The model developed and validated in this paper has been subsequently employed to investigate the grasp force and conformability of the FRE fingers in simulation. Then, a modified FRE gripper was designed, and the fabricated gripper was tested to grasp objects of various shapes and sizes. The proposed FRE gripper could significantly improve the load capacity in practice, and better tolerate fast robotic maneuvers. Moreover, it is better suited for bin picking scenarios.

To the best of our knowledge, this is the first time that:

- A modeling method for FRE fingers integrally made of soft material has been proposed that considers continuum behavior of all beams using continuum Cosserat rod formulation and accurately estimates their shape (maximum error of 2.5 %).
- A novel mounting adaptor design for the FRE fingers has been developed that could improve their load capacity up to 150 % while providing more stable grasps and enhanced bin picking capabilities.

2. Modeling and analysis

The FRE gripper structure, as shown in Fig. 1(a), consists of three sections: (i) the soft FRE fingers that directly contact the object and conform to its shape in reaction to the contact force; (ii) the mounting adaptor, which is a rigid element and determines the boundary conditions of the FRE finger and can affect its conforming shape and grasp forces; and (iii) the actuation mechanism which provides the lateral movements for the fingers. This section focuses on the modeling and analysis of the FRE fingers, considering the governing boundary conditions.

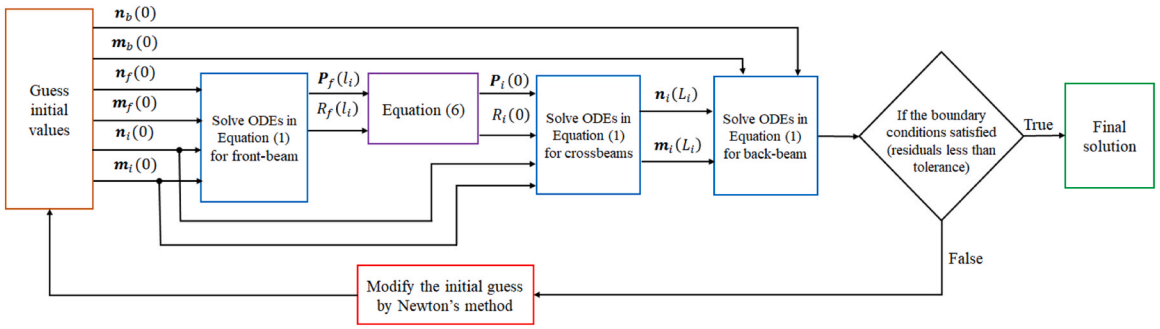

Fig. 2. Flowchart of the proposed modelling method.

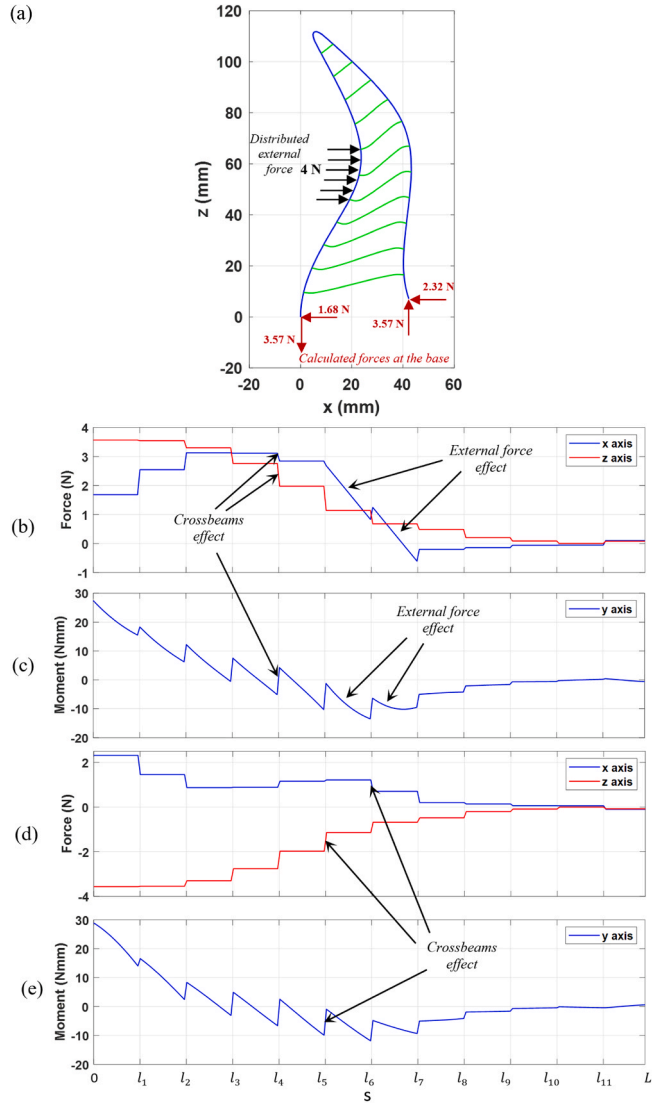

Fig. 3. (a) The estimated shape of the FRE finger after applying a distributed external force, with the calculated (b) internal force and (c) moment in the front-beam, and the (d) internal force and (e) moment of the back-beam.

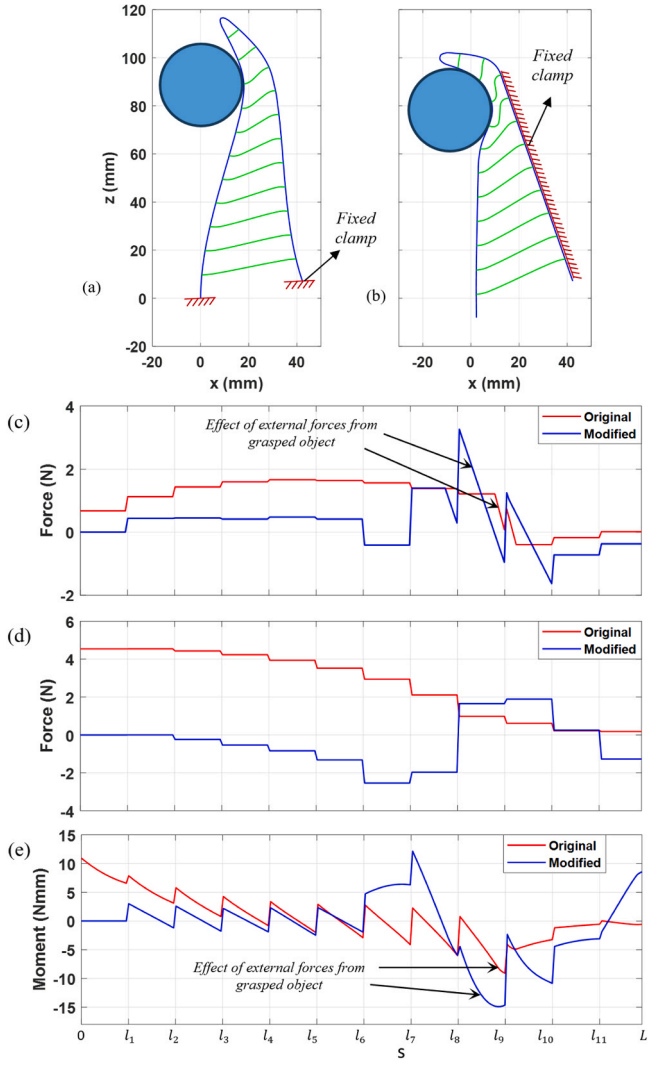

Fig. 4. Simulated finger shape after gripping a circular object with (a) the original gripper and (b) the modified gripper, with the internal forces of the front beam in (c) the *x* axis, and (d) the *z* axis, and (e) the internal moments in *y* axis.

2.1. FRE modeling

Each FRE finger includes two main beams (front- and back-beams), and several crossbeams (Fig. 1(b)). Each beam is independently described by the system of differential equations based on the Cosserat rod theory [33,34]. The shape of the beams can be described as their centerline curve Cartesian position in space $\boldsymbol{P}(s) \in \mathbb{R}^3$, and the rotation matrix of their material orientation $\boldsymbol{R}(s) \in \mathrm{SO}(3)$, as functions of the arc-length of the beam $s \in [0\ L]$ (L is the length of undeformed beam). The static model of the elastic beam based on the Cosserat rod theory is described by the following ODEs:

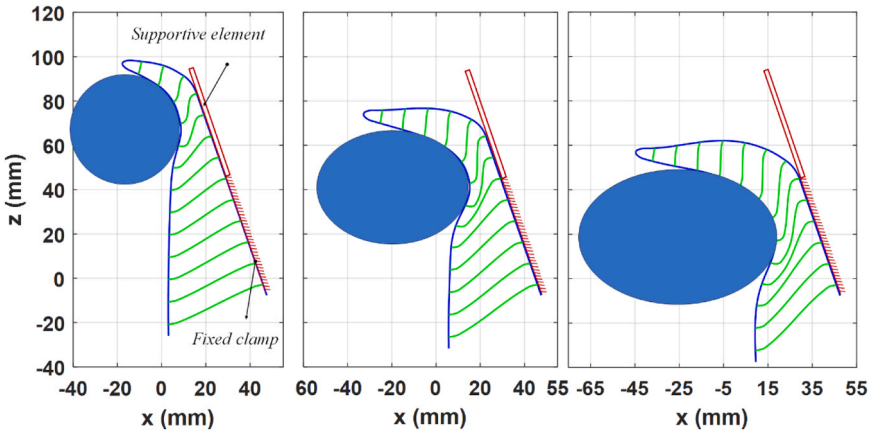

Fig. 5. Simulated finger shape with the modified boundary conditions.

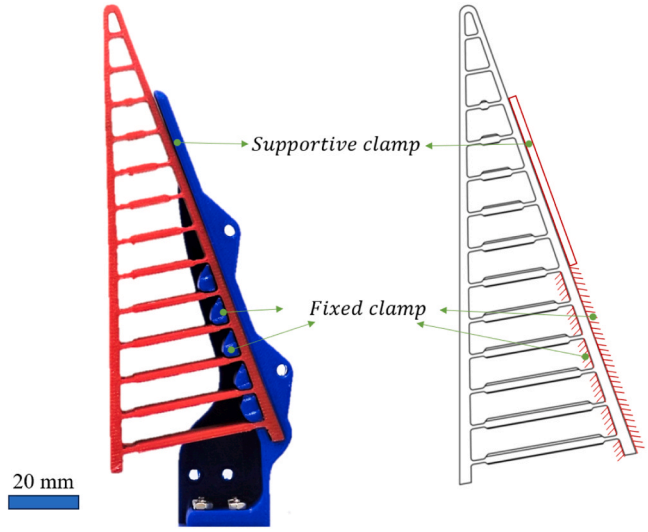

Fig. 6. A FRE finger with the modified mounting adaptor and schematic of its boundary conditions.

$$\begin{aligned}
\dot{\boldsymbol{P}} &= \boldsymbol{R}\left(\boldsymbol{K}_{se}{}^{-1}\boldsymbol{R}^{\mathrm{T}}\boldsymbol{n} + \boldsymbol{\nu}^{*}\right),\\
\dot{\boldsymbol{R}} &= \boldsymbol{R}\left(\boldsymbol{K}_{bt}{}^{-1}\boldsymbol{R}^{\mathrm{T}}\boldsymbol{m}\right)^{\wedge},\\
\dot{\boldsymbol{n}} &= -\boldsymbol{\rho},\\
\dot{\boldsymbol{m}} &= -\dot{\boldsymbol{P}} \times \boldsymbol{n} - \boldsymbol{\mu},
\end{aligned} \tag{1}$$

where the dot denotes a derivative with respect to s, and $(.)^{\wedge}$ represents the mapping from $\mathbb{R}^3$ to $\mathfrak{so}(3)$ [35]. $\boldsymbol{n}(s)$ and $\boldsymbol{m}(s)$ are the internal force and moment vectors in the global coordinate frame, respectively. $\boldsymbol{\rho}$ and $\boldsymbol{\mu}$ correspond to the force and moment variations along the beams. $\boldsymbol{\nu}^{*}$ is the kinematic variable of the beam in a stress-free reference state [33]. $\boldsymbol{K}_{se}$ is the stiffness matrix for shear and extension, and $\boldsymbol{K}_{bt}$ represents the stiffness matrix for bending and twisting, defined as follow:

$$\boldsymbol{K}_{se} = A(s)\begin{bmatrix} G & 0 & 0\\ 0 & G & 0\\ 0 & 0 & E \end{bmatrix},$$

$$\boldsymbol{K}_{bt} = \begin{bmatrix} EI_{xx}(s) & 0 & 0\\ 0 & EI_{yy}(s) & 0\\ 0 & 0 & G(I_{xx}(s) + I_{yy}(s)) \end{bmatrix}, \tag{2}$$

where $A(s)$ is the cross-sectional area of the beam, E and G are the Young's modulus and the Shear modulus, respectively. $I_{xx}(s)$ and $I_{yy}(s)$ are the second moments of area of the beam cross section about the principal axes. In the following, to describe the variables in Eq. (1), we use the suffix f for the front-beam, b for the back-beam, and i is for the ith crossbeam, where $i = 1$ to n.

In a FRE finger structure, each crossbeam is clamped to the main beams at both ends. The ith crossbeam at its base ($s_i = 0$), is fixed to the front-beam at the arc length $s_f = l_i$. Moreover, the ith crossbeam at its end ($s_i = L_i$), is fixed to the back-beam at the arc length $s_b = l_i$. Therefore, the forces and moments at the base and end of the ith crossbeam will be applied to the main beams at the arc length l_i. Thus, for $\boldsymbol{\rho}$ and $\boldsymbol{\mu}$ one can obtain:

$$\begin{aligned}
\boldsymbol{\rho}_f &= \boldsymbol{F}_c + \sum_{i=1}^{n} \boldsymbol{n}_i(0)\delta(s_f - l_i),\\
\boldsymbol{\mu}_f &= \sum_{i=1}^{n} \boldsymbol{m}_i(0)\delta(s_f - l_i),\\
\boldsymbol{\rho}_b &= \sum_{i=1}^{n} \boldsymbol{n}_i(L_i)\delta(s_b - l_i),\\
\boldsymbol{\mu}_b &= \sum_{i=1}^{n} \boldsymbol{m}_i(L_i)\delta(s_b - l_i),\\
\boldsymbol{\rho}_i &= \boldsymbol{0},\ \boldsymbol{\mu}_i = \boldsymbol{0},\ \text{for}\ \ i = 1 \ldots n,
\end{aligned} \tag{3}$$

where $\boldsymbol{F}_c$ is the distributed contact force vector applied to the front-beam by gripping an object, and $\delta(.)$ is the Dirac delta function.

2.2. Boundary conditions and computation method

Each beam in the FRE finger was described by the system of differential Eq. (1). However, the boundary conditions of the system of equations are coupled because of the physical constraints inherent in the finger structure. In the following, the governing boundary conditions for the beams are mentioned.

The bases of the main beams are clamped to the rigid mounting adaptor (Fig. 1(b)). So, the position and orientation (pose) of their base ($\boldsymbol{P}_f(0)$, $\boldsymbol{R}_f(0)$, $\boldsymbol{P}_b(0)$ and $\boldsymbol{R}_b(0)$) are known from the mounting adaptor design. Moreover, the ends of the main beams are clamped together and so the following boundary condition equations for the end pose of the main beams can be obtained:

$$\begin{aligned}
&\boldsymbol{P}_f(L_f) = \boldsymbol{P}_b(L_b),\\
&[\log(R_f(L_f)R_b(L_b))]^{\vee} = \boldsymbol{0}.
\end{aligned} \tag{4}$$

where $\log()$ is the matrix natural logarithm which maps SO(3) to $\mathfrak{so}(3)$, and $(.)^{\vee}$ represents the mapping from$\mathfrak{so}(3)$ to $\mathbb{R}^3$. The following conditions of static equilibrium must also hold at the end of the main beams:

$$\boldsymbol{n}_f(L_f) = \boldsymbol{n}_b(L_b),$$

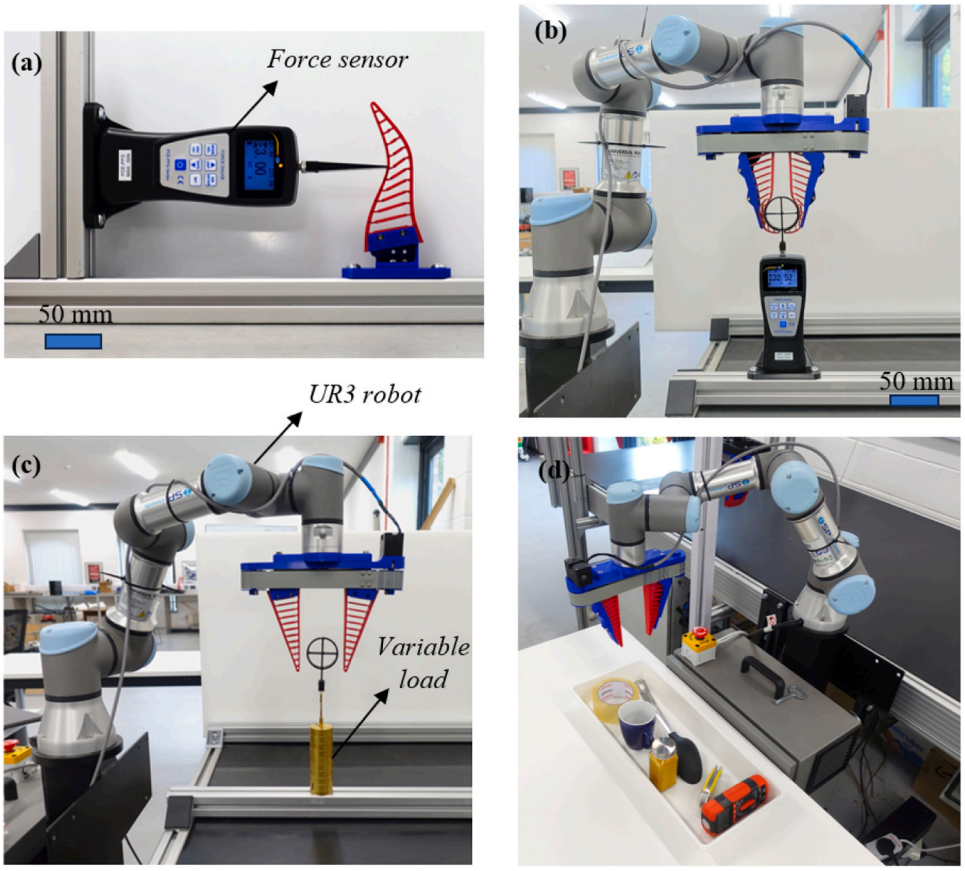

Fig. 7. The experimental setup for (a) model validation, (b) measuring the release forces, (c) evaluating the load capacity, and (d) the grasp stability of grippers.

$$\boldsymbol{m}_f(L_f) = \boldsymbol{m}_b(L_b), \tag{5}$$

Since the base of the ith crossbeam is clamped to the front-beam at the arclength l_i, thus the following boundary condition equations for the base of all the crossbeams can be obtained:

$$\boldsymbol{P}_i(0) = \boldsymbol{P}_f(l_i),$$

$$[\log(R_i(0)R_f(l_i))]^\vee = \boldsymbol{0}, \text{for} i = 1\ldots n. \tag{6}$$

Moreover, the end of each crossbeam ($s = L_i$) is clamped to the back-beam and therefore, for the end pose of the crossbeams, one can obtain:

$$\boldsymbol{P}_i(L_i) = \boldsymbol{P}_b(l_i),$$

$$[\log(R_i(L_i)R_b(l_i))]^\vee = \boldsymbol{0}, \text{for} i = 1\ldots n. \tag{7}$$

However, to solve the ODEs in Eq. (1) and determine the shape of the deformed beams, the forces and moments at the base of the main beams and crossbeams are still unknown. The shooting method provides an effective way to solve the systems of equations subject to the coupled boundary conditions, by changing the boundary value problem into an initial value problem. In this procedure, the unknown boundary conditions are guessed. Each system of beam equations is numerically integrated from $s = 0$ to L, as an initial value problem using a standard numerical routine, and the boundary condition equations are subsequently evaluated. The algorithm solves the system of equations through the following steps:

1. Calculate the system of ODEs (Eq. (1)) for the front-beam, by guessing the forces and the moments at the base of front-beam ($\boldsymbol{n}_f(0)$ and $\boldsymbol{m}_f(0)$), and at the base of all crossbeams ($\boldsymbol{n}_i(0)$ and $\boldsymbol{m}_i(0)$ for $i = 1\ldots n$).
2. Compute the ODEs for all crossbeams having pose of their base from Eq. (6) and using the pose of front-beam from the first step.
3. Calculate the ODE equations for the back-beam having the forces and moments at the end of the crossbeams ($\boldsymbol{n}_i(L_i)$ and $\boldsymbol{m}_i(L_i)$) from the second step.
4. Evaluate the boundary conditions given in the Eqs. (4), (5) and (7).
5. Run an optimization loop that iteratively updates the guessed values until the boundary conditions are satisfied within an appropriate tolerance.

The flowchart describing the proposed modelling method is shown in Fig. 2. This modeling method can be used for the analysis and optimization of FRE grippers by altering model parameters, beam arrangements, or mounting methods. Changes in beam configurations or mounting methods may affect the boundary conditions, requiring minor adjustments to the boundary condition rules. The performance of the proposed model is evaluated in the "Experimental study" section of this paper.

2.3. Simulation and analysis

To analyze the FRE finger behavior and the internal forces, the proposed algorithm was implemented in MATLAB with an initial guess of zero for all unknown conditions. The simulation results for applying a horizontal distributed force of 4 N in the x direction are given in Fig. 3. The estimated shape of the deformed finger is shown in Fig. 3(a), and the calculated internal forces and moments for both front and back-beams are given in Fig. 3(b)-(e).

The calculated forces at the base of the front-beam include an upward force, and a horizontal force in the opposite direction of the external force. The external distributed force causes an inclined varia-

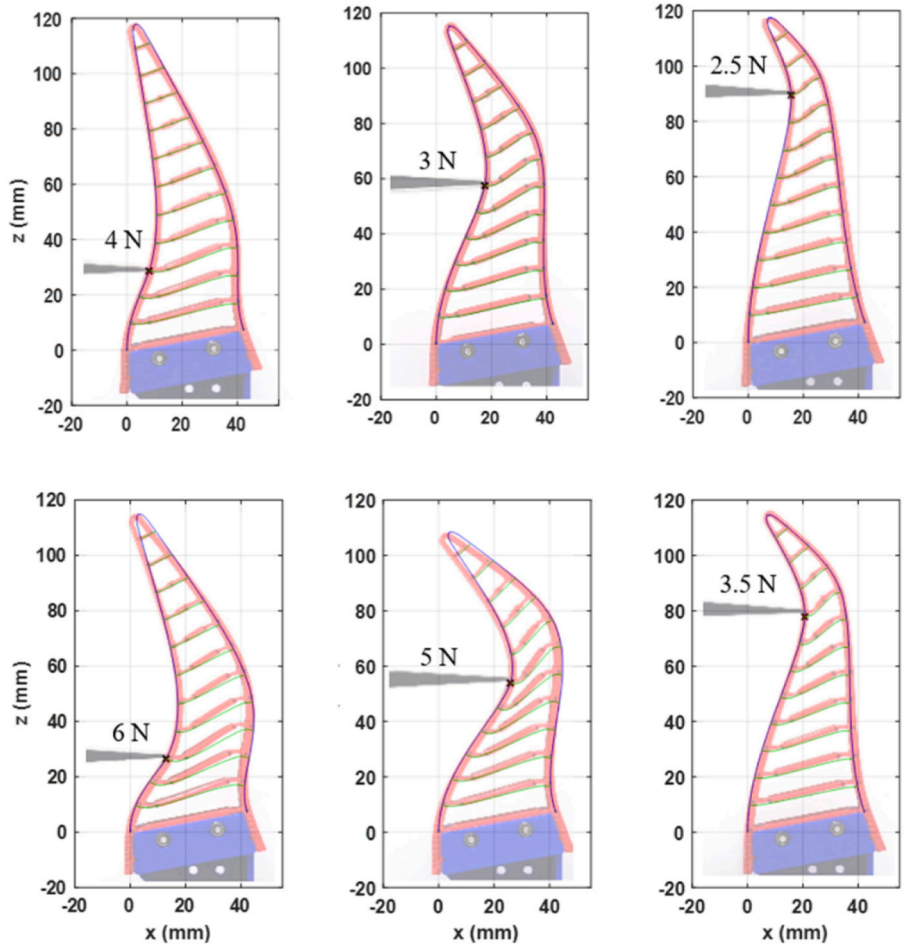

Fig. 8. Comparison of the estimated shape and the actual shape of FRE finger with original mounting adaptor.

tion in the calculated internal force of the front-beam at the arc lengths where the force is applied (from $s = l_5$ to l_7), in the x axis (see Fig. 3(b)). The external force can also cause a curved variation in the calculated internal moments of the front-beam as shown in Fig. 3(c). The breakpoints in these graphs show the applied forces and moments from the crossbeams. Therefore, the jagged shapes in internal force and moment graphs arise from the concentrated and distributed forces and moments acting on the beams, including the distributed contact force ($\boldsymbol{F}_c$) and the concentrated reactions from the crossbeams ($\boldsymbol{n}_i(0)$, $\boldsymbol{n}_i(L_i)$, $\boldsymbol{m}_i(0)$ and $\boldsymbol{m}_i(L_i)$).

From Fig. 3, it can be concluded that the crossbeams apply mostly negative forces along the x and z axes, and negative moments along the y axis, to the front-beam. These forces and moments from the crossbeams cause the front-beam to bend in the opposite direction of the external contact force, rather than in its direction. This causes the front-beam to envelop the object in reaction to the contact force and grip the object.

The crossbeams apply the same forces, but in the opposite direction to the back-beam. However, the applied moments to the back-beam, like the front-beam, are negative moments along the y axis (see Fig. 3(d) and (e)). Therefore, the back-beam bends in the opposite direction of the external force and moves backward, in reaction to the internal forces and moments from the crossbeams. The coupled mechanics of all beams determine the shape of the deformed FRE finger. The next section describes the modified design based on the analyzed internal forces and moments.

While finite element methods are widely used for analyzing soft robotic structures, their accuracy can vary significantly depending on solver settings, meshing strategies, and the software employed. The Cosserat rod-based mathematical model proposed in this study offers a physically interpretable framework that enables accurate prediction of finger deformation, as well as internal forces and moments. It allows for fast parametric studies and design optimization without the need for time-intensive meshing or complex numerical solvers. The model is validated against experimental results obtained from real FRE fingers, as detailed in the 'Experimental Study' section, demonstrating strong predictive performance and offering clear advantages for design iteration and boundary condition analysis.

3. Design modification

The analysis and conclusions presented in this section are derived from systematic investigations using the proposed Cosserat rod-based model. By simulating various design configurations and boundary conditions, the model enables detailed evaluation of internal force interactions and deformation behaviors, which were not readily accessible through traditional experimental methods alone.

To have a more stable grasp and reach a higher load capacity, given the same finger material (unchanged friction coefficient), a greater contact surface between the object and the finger, as well as increased contact forces, is required. Therefore, the front-beam needs to bend more around the object and apply greater contact forces to it. To accomplish this, more force must be exerted by the crossbeams onto the front-beam. Different arrangements of the crossbeams were investigated to increase the internal forces of the crossbeams and improve the grasp stability as well as the load capacity of the FRE fingers. But changing the crossbeam configuration did not have a significant effect on the desired properties. So, different mounting adaptor designs, by changing the boundary conditions of the finger, were investigated in simulation. The

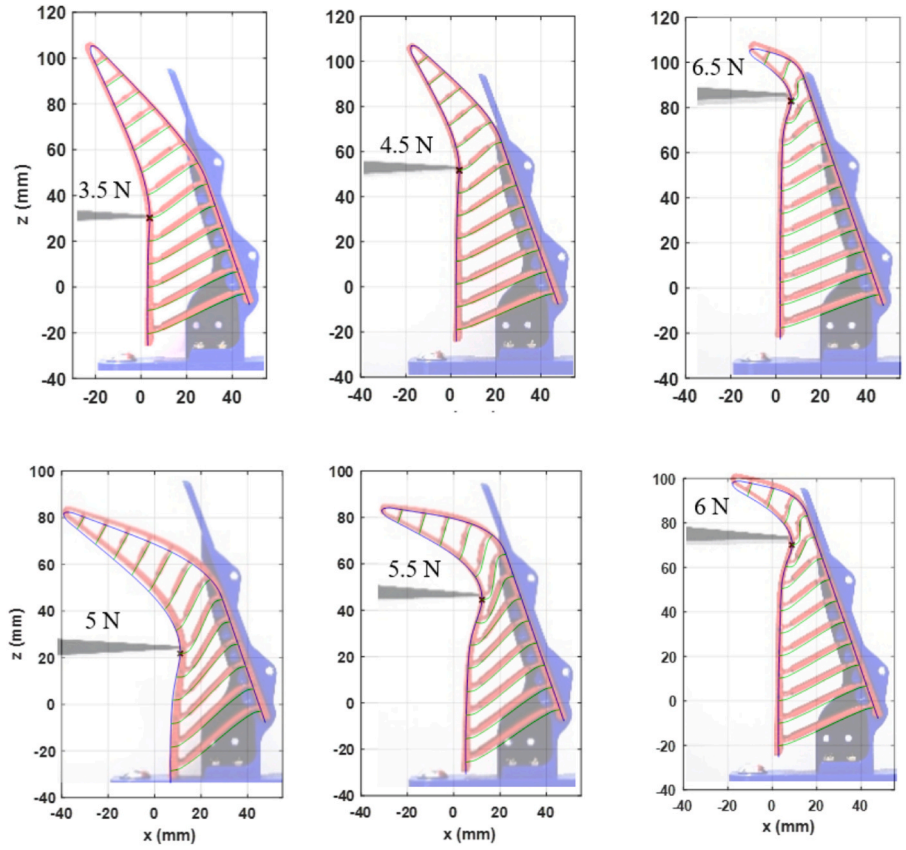

Fig. 9. Comparison of the estimated shape and the actual shape of FRE finger with the modified mounting adaptor.

Table 1
Results from first test: shape estimation error results.

Mounting adaptor	Applied force		Shape estimation results			
	(N)	Contact arc length	RMS error*		Max error*	
			(*mm*)	%	(*mm*)	%
Original	4	l_5	0.79	0.66	1.91	1.59
	3	l_8	0.66	0.55	1.54	1.28
	2.5	l_{11}	0.84	0.70	1.77	1.47
	6	l_5	1.11	0.93	2.56	2.13
	5	l_8	1.30	1.08	2.91	2.42
	3.5	l_{10}	0.84	0.70	1.43	1.19
Modified	3.5	l_6	1.02	0.85	2.33	1.94
	4.5	l_8	0.72	0.60	1.21	1.01
	6.5	l_{11}	1.06	0.88	1.99	1.65
	5	l_6	0.85	0.70	1.56	1.30
	5.5	l_8	1.01	0.84	2.23	1.85
	6	l_{10}	0.74	0.62	1.71	1.42

* The error is presented in *mm* and in % with respect to the length of the FRE finger.

results showed that a proper mounting adaptor can considerably affect the internal forces applied by the crossbeams and influence the resulting shape of the front-beam.

As mentioned in the previous section, to reach the required grasp specifications, it is necessary that the front-beam bends properly around the object to prevent it from being released by gravitational or inertial forces. To increase the internal forces in the crossbeams, the back-beam needs to exert more force on the crossbeams in the direction opposite to the contact force. However, since the back-beam is flexible, its reaction forces are limited as it moves backward in response to the internal forces from the crossbeams. Restricting the movement of the back-beam by altering the governing boundary conditions can significantly increase its reaction forces. A supportive element can provide the necessary boundary condition. Additionally, releasing the base of the front beam from the mounting adapter allows it to bend more easily in response to external contact forces. These principles form the design foundation of the modified mounting adapter.

Fig. 4(a) shows a finger with the original mounting adaptor after gripping an 18 mm circular object. By releasing the base of the front-beam and restricting the deformation of the back-beam, the finger shape changes to Fig. 4(b). Comparison of the two finger shapes shows that with the new boundary condition, the fingertip bends more, which can provide a more stable grasp for an object with the same dimensions. The internal forces and moments of the front-beam for both fingers are given in Fig. 4(c)-(e). The results show that the average forces applied from crossbeams to the front-beam increased in the modified design by 285 % in the x axis, and by 16 % in the z axis. As a result, the front-beam in the new design better envelops the object and the applied force to the object increased by 260 %.

Moreover, the simulations revealed that for gripping larger objects, a shorter length of the back-beam must be fixed as shown in Fig. 5. Therefore, based on the desired boundary conditions for the finger, in the modified design of the mounting adaptor, the back-beam is fixed in some parts and a supportive element restricts the backward movement of some other parts.

The portion of the back-beam to be clamped was determined through simulation analysis to ensure that the clamped part does not affect the bending of the FRE finger while gripping objects of various sizes. Fig. 6 shows the modified mounting adaptor, as well as the schematic for its boundary condition.

4. Experimental study

This section investigates the performance of the proposed modeling

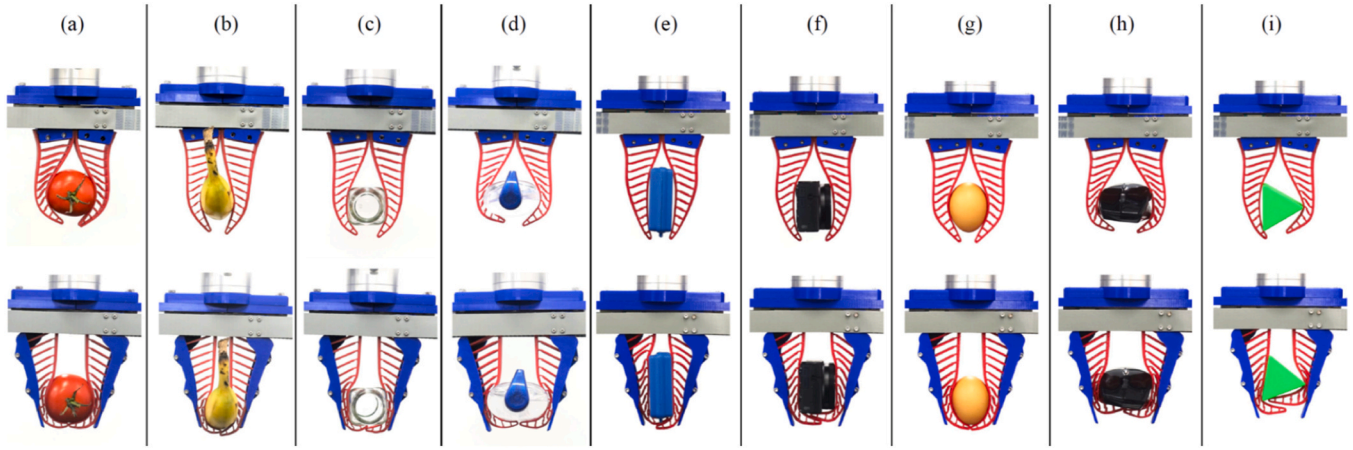

Fig. 10. Results from second test: comparison of finger shapes after gripping (a) a tomato, (b) a banana, (c) a glass container, (d) a plastic pump dispenser, (e) a rectangular container, (f) a digital camera, (g) an egg, (h) a computer mouse, and (i) a triangular container.

Table 2
Results from third test: releasing forces results.

	Object diameter (mm)	Measured force (N)						Improvement (%)
		Original gripper			Modified gripper			
		Min	Avr	Max	Min	Avr	Max	
Finger−1	35	5.9	6.0	6.2	17.9	18.4	19.1	205
	50	8.7	8.85	8.9	21.9	22.5	22.9	154
	65	12.1	12.2	12.2	26.7	27.1	27.3	122
Finger−2	35	7.8	8.0	8.6	22.3	24.0	24.9	200
	50	10.3	10.7	11.0	28.3	29.4	30.3	174

Table 3
Results from fourth test: load capacity results.

	Maximum load (g)		Improvement (%)
	Original gripper	Modified gripper	
Finger−1	600	1600	166.6
Finger−2	700	1800	157.1

method and the modified FRE gripper experimentally.

4.1. Experimental procedure

The FRE fingers are made of NinjaFlex filament and printed using a LulzBot TAZ-6 printer. Two different FRE finger designs developed by Festo are used in the experimental tests: the DHAS-GF-120-U-BU, referred to here as Finger-1, with a height of 120 mm, and the DHAS-GF-80-U-BU, referred to here as Finger-2, with a height of 80 mm. The actuation mechanism used in the experiments utilizes a Dynamixel XH430-W350-R motor as actuator and T5 timing belt and pulley as power transmission system. A force sensor PCE-PFG-50 is used to measure the applied forces to the fingers, as well as the grasp forces. To examine the performance of the mathematical modeling method, the estimated shapes of the finger after applying different forces in different positions are compared with the reconstructed ones using two cameras (DSC-RX100M4, Sony) in stereo configuration and using a Direct Linear Transformation (DLT) approach [36]. In the experiments, the Root Mean Square (RMS) error for the shape estimation is obtained with the following equation:

$$e_{rms} = \sqrt{\frac{1}{N}\sum_{1}^{N}(\boldsymbol{P}-\overline{\boldsymbol{P}})^{\mathrm{T}}(\boldsymbol{P}-\overline{\boldsymbol{P}})}. \tag{8}$$

where N is the number of the measured points and $\overline{\boldsymbol{P}}$ is the marker position reconstructed with the DLT. Five different types of tests have been executed in this research as described below.

In the first test, to validate the performance of the proposed modeling method, the predicted shape of the model is compared with the real one using the reconstructed marker positions measured with the vision system. A blade printed using PLA was used to apply concentrated forces to the finger and was mounted on the force sensor. Fig. 7(a) shows the setup for this test.

The second test compares the conformability of the grippers with different object shapes. This test visually compares the grippers when grasping delicate objects of various sizes and shapes.

The third test compares the release forces of the grippers. For this test, the grippers are mounted on a UR3 arm in a vertical configuration as shown in Fig. 7(b). Then, circular objects with diameters of 35, 50 and 65 mm are grasped with both grippers, while the circular objects were fixed to the force sensor from below. Then, the robot moves upward and since the object is fixed to the force sensor, the gripper releases it during this movement. The sensor registers maximum force during each test.

The fourth test investigates the load capacity of the grippers. In this way the grippers, while mounted on the robotic arm, grasp a circular object of diameter 50 mm, and try to move it upward. The circular object is connected to a variable load as shown in Fig. 7(c).

In the fifth test, to examine the grasp stability, the grippers are used to pick and place different objects with various shapes and sizes (Fig. 7 (d)). The UR3 arm moves at its maximum speed (1 m/s), during this test.

4.2. Results and discussion

Fig. 8 shows the results for the first test when different amounts of horizontal force are applied at different arc lengths of the front-beam of the FRE finger with the original mounting adaptor. This figure compares

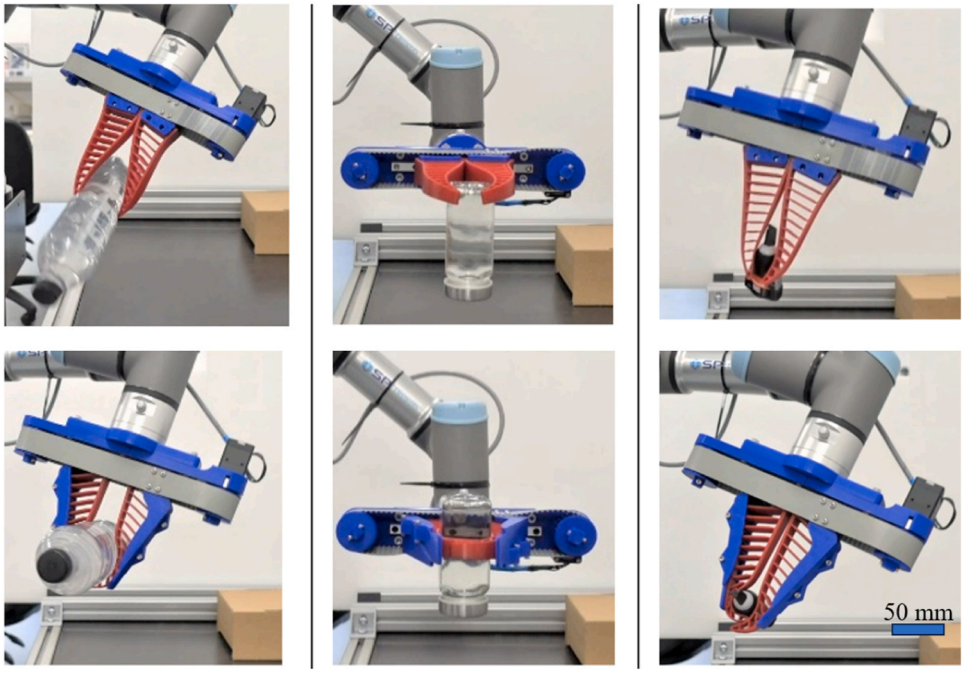

Fig. 11. Results from fifth test: Comparison of the grasp stability of the grippers.

the actual shape of the finger with the simulated one using the proposed model. Similar results for the finger with the modified mounting adaptor are given in Fig. 9. As it appears from visual inspection, the proposed method can properly estimate the shape of the finger under the contact of different external forces. Table 1 summarizes the RMS and the maximum values of the shape estimation error in both millimeters and as a percentage of the finger's length. From the results, it can be concluded that the maximum prediction error of the proposed model is confined within 2.5 %.

The results of the second test are shown in Fig. 10, which compares the finger shapes after gripping delicate objects of various shapes and sizes. The modified FRE gripper was evaluated using objects with circular, rectangular, ovoid, triangular, and asymmetric geometries. The proposed design consistently demonstrated improved conformability across all tested shapes, confirming that the structural modifications enhance the gripper's versatility rather than limiting it. As illustrated in the figure, the modified design more effectively envelops a wide range of object geometries, resulting in more stable and secure grasps.

To measure the releasing force of the grippers, the third test is repeated 5 times for each circular object and each gripper. Two FRE fingers of different sizes (Finger-1 and Finger-2) were examined in this test. Table 2 summarizes the maximum, minimum, and average values for the measured forces. The results revealed that the modified design significantly improves the release forces for both fingers. The improvement for different object sizes is more than 120 %, and for smaller objects, this improvement is even more considerable. The accompanying video (supplementary file 1) demonstrates this test.

Supplementary material related to this article can be found online at doi:10.1016/j.sna.2025.116711

To evaluate the load capacity of the grippers, in the fourth test, the loads were increased in steps of 100 g. The accompanying video (Supplementary File 2) demonstrates this test, and Table 3 summarizes the maximum load lifted by each gripper and finger. The original gripper with both fingers was unable to lift an 800 g load. However, the modified gripper could tolerate loads up to 1800 g. The load capacity improvement for each finger is also given in this table. From the results, the load capacity in the proposed design has increased by more than 150 %.

Supplementary material related to this article can be found online at doi:10.1016/j.sna.2025.116711

In the last (fifth) test, each gripper was used to pick and place a plastic bottle of water (545 g), a glass container filled with water (255 g), and a small glue container (18 g), as given in Fig. 11. Each test was repeated five times. The accompanying video (supplementary file 3) demonstrates this test. The original gripper was unable to successfully pick and place these challenging objects and failed in all tests. However, the modified gripper reliably performed all pick and place tests by providing a stable grasp. Moreover, we compared both grippers in a bin picking scenario where mostly the gripper's tip comes in contact with the object. This test was performed twice, and as demonstrated in the accompanying video (Supplementary File 4) demonstrates, the proposed gripper successfully picked up and stably moved all six objects both times (the objects shown in Fig. 7(d)). However, the conventional gripper was able to pick up and stably move only one of the objects in both repetitions. From these results, it is evident that the proposed method can substantially improve the grasp stability of FRE grippers for pick-and-place scenarios, which are common in most industrial applications.

Supplementary material related to this article can be found online at doi:10.1016/j.sna.2025.116711

It is important to note that the goal of this study was to achieve improved grasp stability and load capacity while preserving the softness and flexibility of the original finger material. Increasing the material stiffness would reduce conformability and contact surface area, while potentially increasing localized stresses, which can compromise the safe handling of delicate objects such as eggs. The proposed approach maintains the finger's flexibility and enhances performance by modifying the boundary conditions and internal force distributions, enabling safer and more reliable grasping across a variety of object types.

5. Conclusion

This research focused on significantly improving the load capacity, grasp stability, and addition of bin picking capability to FRE grippers while maintaining or enhancing their positive features, such as adapting to various shapes and delicately grasping a wide range of objects. We aimed to preserve the softness of the fingers by avoiding changes to the material properties. To analyze the FRE fingers fabricated integrally

with soft material, an accurate modeling method was proposed that considers the continuum behavior of all beams in these fingers. The simulation analysis revealed that changing the boundary conditions results in a significant increase in grasp forces and conformity performance. Experimental investigations revealed that the modified FRE gripper design based on the new boundary conditions significantly improves the load capacity and grasp stability. This performance improvement comes at the expense of specific optimizations. If clear design specifications are known, our modeling approach can help identify the optimal beam parameters (material and geometrical). The developed gripper can be utilized for different applications where reliable movement of delicate objects is needed. Examples include sorting, packaging, and palletizing various goods in warehouse or retail automation, as well as harvesting or handling crops in agricultural settings.

CRediT authorship contribution statement

Mohammad Sheikh Sofla: Writing – original draft, Validation, Software, Methodology, Conceptualization, Formal analysis, Investigation. **Hanita Golshanian:** Validation. **Elizabeth I. Sklar:** Writing – review & editing, Supervision. **Marcello Calisti:** Writing – review & editing, Supervision, Funding acquisition, Conceptualization.

Declaration of Competing Interest

The authors declare the following financial interests/personal relationships which may be considered as potential competing interests. Mohammad Sheikh Sofla reports financial support was provided by Forestry Commission. If there are other authors, they declare that they have no known competing financial interests or personal relationships that could have appeared to influence the work reported in this paper.

Acknowledgements

This work was supported by the UK Forestry Commission's Tree Production Innovation Fund under grand: Intelligent Singulating and Labelling of Developing Trees Using Robotics (ISILDUR), #TPIF_38.

Data availability

Data will be made available on request.

References

[1] Y.A. AboZaid, M.T. Aboelrayat, I.S. Fahim, A.G. Radwan, Soft robotic grippers: a review on technologies, materials, and applications, Sens. Actuators A Phys. 372 (April) (2024) 115380, https://doi.org/10.1016/j.sna.2024.115380.
[2] T. Hu, X. Lu, D. Xu, A dual-mode and enclosing soft robotic gripper with stiffness-tunable and high-load capacity, Sens. Actuators A Phys. 354 (December 2022) (2023), https://doi.org/10.1016/j.sna.2023.114294.
[3] M.S. Sofla, M.J. Sadigh, S.M. Hadi Sadati, C. Bergeles, M. Zareinejad, Sliding-surface dynamic control of a continuum manipulator with large workspace, Control Eng. Pr. 141 (April) (2023) 105680, https://doi.org/10.1016/j.conengprac.2023.105680.
[4] M.S. Sofla, H. Golshanian, S.Vishnu Rajendran, E.Amir Ghalamzan, Soft Acoustic Curvature Sensor: Design and Development, IEEE Robot. Autom. Lett. 9 (11) (2024) 9518–9525, https://doi.org/10.1109/LRA.2024.3460429.
[5] C. Girerd, A. Alvarez, E.W. Hawkes, T.K. Morimoto, Material scrunching enables working channels in miniaturized vine-inspired robots, IEEE Trans. Robot 40 (2024) 2166–2180, https://doi.org/10.1109/TRO.2024.3370088.
[6] Q. Wei, H. Xu, F. Sun, F. Chang, S. Chen, X. Zhang, Biomimetic fiber reinforced dual-mode actuator for soft robots, Sens. Actuators A Phys. 344 (April) (2022), https://doi.org/10.1016/j.sna.2022.113761.
[7] M. Xu, G. Wang, C. Rong, Fiber-reinforced flexible joint actuator for soft arthropod robots, Sens. Actuators A Phys. 340 (April) (2022) 113522, https://doi.org/10.1016/j.sna.2022.113522.
[8] W. Xu, H. Zhang, H. Yuan, B. Liang, A compliant adaptive gripper and its intrinsic force sensing method, IEEE Trans. Robot 37 (5) (2021) 1584–1603, https://doi.org/10.1109/TRO.2021.3060971.
[9] R. Chen, et al., Bio-Inspired Shape-Adaptive Soft Robotic Grippers Augmented with Electroadhesion Functionality, Soft Robot 6 (6) (2019) 701–712, https://doi.org/10.1089/soro.2018.0120.
[10] K. Elgeneidy, P. Lightbody, S. Pearson, G. Neumann, Characterising 3D-printed soft fin ray robotic fingers with layer jamming capability for delicate grasping, RoboSoft 2019 - 2019 IEEE Int. Conf. Soft Robot (2019) 143–148, https://doi.org/10.1109/ROBOSOFT.2019.8722715.
[11] O. Pfaff, S. Simeonov, I. Cirovic, and P. Stano, "Application of finray effect approach for production process automation," Ann. DAAAM Proc. Int. DAAAM Symp., vol. 22, no. 1, pp. 1247–1248, 2011, doi: 10.2507/22nd.daaam.proceedings.608..
[12] C.V. Ince, J. Geggier, A. Raatz, Fin Ray gripper for handling of high temperature hybrid forging objects, Procedia CIRP 106 (March) (2022) 114–119, https://doi.org/10.1016/j.procir.2022.02.164.
[13] "Multi choice gripper," 2014. [Online]. Available: ⟨https://www.festo.com/net/SupportPortal/Files/333986/Festo_MultiChoiceGripper_en.pdf⟩.
[14] L. Kölle, O. Schwarz, Bionic forceps for the handling of sensitive tissue, Curr. Dir. Biomed. Eng. 2 (1) (2016) 91–93, https://doi.org/10.1515/cdbme-2016-0023.
[15] J.M. Gandarias, J.M. Gómez-de-Gabriel, A.J. García-Cerezo, Enhancing perception with tactile object recognition in adaptive grippers for human-robot interaction, Sens. (Switz.) 18 (3) (2018), https://doi.org/10.3390/s18030692.
[16] I. Hussain, et al., Design and prototype of supernumerary robotic finger (SRF) inspired by fin ray® effect for patients suffering from sensorimotor hand impairment, RoboSoft 2019 - 2019 IEEE Int. Conf. Soft Robot (2019) 398–403, https://doi.org/10.1109/ROBOSOFT.2019.8722748.
[17] D. De Barrie, M. Pandya, H. Pandya, M. Hanheide, K. Elgeneidy, A Deep Learning Method for Vision Based Force Prediction of a Soft Fin Ray Gripper Using Simulation Data, Front. Robot. AI 8 (May) (2021) 1–15, https://doi.org/10.3389/frobt.2021.631371.
[18] W. Crooks, G. Vukasin, M. O'Sullivan, W. Messner, C. Rogers, Fin Ray® effect inspired soft robotic gripper: From the robosoft grand challenge toward optimization (no.NOV), Front. Robot. AI 3 (2016) 1–9, https://doi.org/10.3389/frobt.2016.00070.
[19] J.H. Shin, J.G. Park, D. Il Kim, H.S. Yoon, A Universal Soft Gripper with the Optimized Fin Ray Finger, Int. J. Precis. Eng. Manuf. - Green. Technol. 8 (3) (2021) 889–899, https://doi.org/10.1007/s40684-021-00348-1.
[20] K. Elgeneidy, A. Fansa, I. Hussain, K. Goher, Structural optimization of adaptive soft fin ray fingers with variable stiffening capability, IEEE Int. Conf. Soft Robot. (RoboSoft) (2020) 1–6.
[21] W. Crooks, S. Rozen-Levy, B. Trimmer, C. Rogers, W. Messner, Passive gripper inspired by Manduca sexta and the fin ray® effect, Int. J. Adv. Robot. Syst. 14 (4) (2017) 1–7, https://doi.org/10.1177/1729881417721155.
[22] C. Armanini, I. Hussain, M.Z. Iqbal, D. Gan, D. Prattichizzo, F. Renda, Discrete Cosserat Approach for Closed-Chain Soft Robots: Application to the Fin-Ray Finger, IEEE Trans. Robot 37 (6) (2021) 2083–2098, https://doi.org/10.1109/TRO.2021.3075643.
[23] X. Shan, L. Birglen, Modeling and analysis of soft robotic fingers using the fin ray effect, Int. J. Rob. Res. 39 (14) (2020) 1686–1705, https://doi.org/10.1177/0278364920913926.
[24] T. Guillon, Y. Dumont, T. Fourcaud, A new mathematical framework for modelling the biomechanics of growing trees with rod theory, Math. Comput. Model 55 (9–10) (2012) 2061–2077, https://doi.org/10.1016/j.mcm.2011.12.024.
[25] F. Boyer, V. Lebastard, F. Candelier, F. Renda, M. Alamir, Statics and Dynamics of Continuum Robots Based on Cosserat Rods and Optimal Control Theories, IEEE Trans. Robot 39 (2) (2023) 1544–1562, https://doi.org/10.1109/TRO.2022.3226112.
[26] M.S. Sofla, S. Vayakkattil, M. Calisti, "Spatial position estimation of lightweight and delicate objects using a soft haptic probe. 2023 IEEE International Conference on Soft Robotics (RoboSoft), IEEE, Singapore, 2023, p. 23199318, https://doi.org/10.1109/RoboSoft55895.2023.10122004.
[27] M.S. Sofla, S. Vayakkattil, M. Calisti, Haptic Localization with a Soft Whisker from Moment Readings at the Base, Soft Robot Published (2024), https://doi.org/10.1089/soro.2023.0098.
[28] O. Weeger, B. Narayanan, L. De Lorenzis, J. Kiendl, M.L. Dunn, An isogeometric collocation method for frictionless contact of Cosserat rods, Comput. Methods Appl. Mech. Eng. 321 (2017) 361–382, https://doi.org/10.1016/j.cma.2017.04.014.
[29] O. Weeger, S.K. Yeung, M.L. Dunn, Isogeometric collocation methods for Cosserat rods and rod structures, Comput. Methods Appl. Mech. Eng. 316 (2017) 100–122, https://doi.org/10.1016/j.cma.2016.05.009.
[30] L.Y. Lee, S.G. Nurzaman, C.P. Tan, Design and Analysis of a Gripper with Interchangeable Soft Fingers for Ungrounded Mobile Robots, Proc. IEEE 2019 9th Int. Conf. Cybern. Intell. Syst. Robot. Autom. Mechatron., CIS RAM 2019 (2019) 221–226, https://doi.org/10.1109/CIS-RAM47153.2019.9095820.
[31] "Adaptive gripper fingers DHAS," 2017. [Online]. Available: ⟨https://www.festo.com/cat/en-gb_gb/data/doc_ENGB/PDF/EN/DHAS_EN.PDF⟩.
[32] C.I. Basson, G. Bright, Geometric Conformity Study of a Fin Ray Gripper Utilizing Active Haptic Control, IEEE Int. Conf. Control Autom. ICCA 2019-July (2019) 713–718, https://doi.org/10.1109/ICCA.2019.8899497.
[33] J. Till, V. Aloi, C. Rucker, Real-time dynamics of soft and continuum robots based on Cosserat rod models, Int. J. Rob. Res. 38 (6) (2019) 723–746, https://doi.org/10.1177/0278364919842269.

[34] D.C. Rucker, R.J. Webster, "Statics and dynamics of continuum robots with general tendon routing and external loading,", IEEE Trans. Robot 27 (6) (2011) 1033–1044, https://doi.org/10.1109/TRO.2011.2160469.
[35] R. Murray, Z. Li, S. Sastry, A mathematical introduction to robotic manipulation, CRC Press, 1994. Vol. 29.
[36] T.L. Hedrick, Software techniques for two- and three-dimensional kinematic measurements of biological and biomimetic systems, Bioinspir. Biomim. 3 (2008), https://doi.org/10.1088/1748-3182/3/3/034001.

Mohammad Sheikh Sofla Mohammad Sheikh Sofla received his B.S. degree from the University of Mazandaran in 2006, his M.Sc. degree from Amirkabir University of Technology in 2009, and his Ph.D. degree from the University of Tehran in 2022, all in Mechanical Engineering. From 2009–2017, he worked as a robotics researcher at the New Technologies Research Centre, Amirkabir University of Technology. He is currently a Postdoctoral Research Associate in Soft/Bioinspired Robotics at the University of Lincoln, UK. His research interests include soft robotics, bioinspired design, dynamic modeling, control engineering, and mechatronics.

Hanita Golshanian received her B.S. degree in Electrical Engineering from the University of Mazandaran in 2006. She worked as a robotics researcher at the New Technologies Research Centre, Amirkabir University of Technology, and is currently a Research Assistant in Robotics and Intelligent Systems at the University of Lincoln, UK. Her research interests include intelligent systems, robotics, and mechatronics.

Elizabeth Sklar is Director of the Lincoln Institute for Agrifood Technology (LIAT) and Professor in Agri-Robotics at the University of Lincoln. Previously she was Head of the Centre for Robotics Research (CoRe) in the Department of Informatics/Engineering at King's College London and earlier at the City University of New York and Columbia University (US). Her research investigates intelligent methodologies for human-robot teaming and data-backed decision making. She has published over 200 peer-reviewed papers, is a founder of the international educational initiative RoboCupJunior and serves on the editorial board of Current Robotics Reports. She has received over £ 38 M in grants as PI or Co-I, from funders including UKRI research councils, Innovate UK, US National Science Foundation and a US-UK Fulbright fellowship. She was the Research Director of the Lincoln Agri-Robotics (LAR) grant, funded by Research England, and is currently Deputy Director of the UKRI AI CDT in Sustainable Understandable agri-food Systems Transformed by Artificial INtelligence (SUSTAIN).

Marcello Calisti (Member, IEEE) Marcello has a PhD in BioRobotics from Scuola Superiore Sant'Anna (2012), a MSc in Biomedical Engineering from the University of Florence (2008), and a BSc in Mechanical Engineering from the University of Perugia (2005). He is currently an Associate Professor of BioRobotics at Scuola Superiore Sant'Anna, and part of the Department of Excellence in Robotics and AI. His research interests span the domains of soft robotics, robot locomotion, and field robotics, encompassing underwater and agricultural robotics. He has been the Principal Investigator of scientific and applied projects funded by IUK, SBRI, BBSRC, NatGeo, and private entities. He was also involved in several European projects regarding soft robotics and underwater robotics. He has been an IEEE Member since 2007 and a National Geographic Explorer since 2017.